Optimization of Radar Search Patterns in Localized Clutter and Terrain Masking under Direction-Specific Scan Update Rates Constraints

Yann Briheche, Frédéric Barbaresco, Fouad Bennis, Damien Chablat

Optimization of Radar Search Patterns in Localized Clutter and Terrain Masking under Direction-Specific Scan Update Rates Constraints

Yann Briheche[1,2,*], Frederic Barbaresco[1], Fouad Bennis[2], Damien Chablat[2]

[1]THALES AIR SYSTEMS, Voie Pierre-Gilles de Gennes, 91470 Limours, France
[2]Laboratoire des Sciences du Numérique de Nantes, UMR CNRS 6004, 44321 Nantes, France
[*]yann.briheche@thalesgroup.com

Abstract: Cognitive radars are systems capable of optimizing emission and processing by exploiting knowledge about environment and operational scenario. Those improvements are achieved by controlling new degrees of freedom offered by modern radar technology. In particular, active phased-array radars can perform bidimensional beam-steering and beam-forming. Those new capabilities allow adaptation of radar search patterns to localized constraints. We present an improvement from our previous set cover approximation for radar search pattern time-budget minimization, accounting for localized constraints of terrain masking and direction-specific scan update rates. The addition of those constraints however does not modify the underlying mathematical structure of the problem, which can be solved using integer programming methods.

Introduction

Multi-function radars usually perform multiple tasks simultaneously, such as scanning, target tracking and identification, clutter mapping, etc. [1–7]. During those tasks, radars gather information about the environment which cognitive radar techniques can use to improve performances by exploiting modern radar capabilities. For example, electronic scanning and numerical processing allow dynamical use of beam-steering, beam-forming, dwell scheduling and waveform processing to adapt to operational requirements. As complex situations can result in system overload, multi-function radars must optimize resources allocation to ensure robust detection. Optimization of the radar search pattern minimizes the required time-budget for radar scanning, thus freeing resources for other tasks.

In the past, several works have explored various approaches for optimization of the radar search pattern: [8, 9] optimized scanning by tiling identical pencil beams over the surveillance space, [10] developed adaptive activation strategies on a pre-designed radar search pattern. Those approaches however do not fully use active radars capabilities to dynamically perform beam-forming. In [11] we presented an approximation of radar search pattern optimization as a set cover problem, defining a flexible and powerful framework for solving this problem. In [12], we presented how localized clutter and multiple missions can be integrated into the optimization problem formulation without changing its mathematical structure.

Set covering is a well-known problem in combinatorial optimization: considering a collection of covers on a set of elements, called the universe, find the smallest subset of this collection whose union covers the universe. The general theoretical problem is known to be NP-difficult [13]. Most optimization algorithms found in the literature are either exact methods based on branch-and-

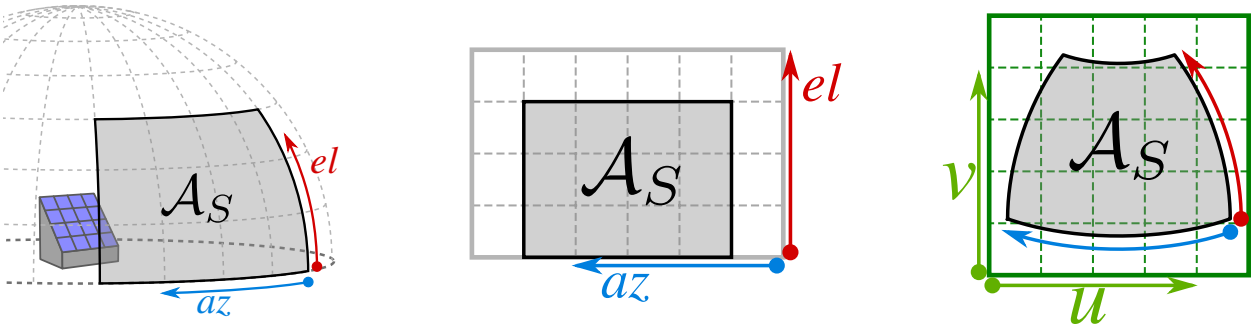

Fig. 1. *Surveillance space in 3D (left), in azimuth/elevation (center), in direction cosines (right)*

bound, approximation heuristics like the greedy algorithm, or evolutionary methods such as simulated annealing or genetic algorithms, see [14] for a recent review of those different approaches. In practice, problems of reasonable size can be efficiently solved using branch-and-bound with linear relaxation for lower bound estimation.

We extend our optimization procedure for radar search pattern time-budget minimization to account for direction specific scan update rate and terrain masking constraints. The first section states the problem, the detection constraints and the radar model. The second section describes the approximation procedure of the problem into combinatorial form. The third section presents the branch-and-bound method used for optimization of the combinatorial problem. The fourth section presents simulation results on a study case.

1. Problem Statement

A *radar search pattern* is a collection of dwells ensuring detection over the surveillance space. An optimal radar search pattern achieves detection using a minimum time-budget. The surveillance space $\mathcal{A}_S$ defines our scanning range in azimuth-elevation coordinates, see Fig. 1:

$$\mathcal{A}_S = [az_{min}, az_{max}] \times [el_{min}, el_{max}] \subset [-\frac{\pi}{2}, \frac{\pi}{2}] \times [0, \frac{\pi}{2}] \tag{1}$$

where az and el are respectively the azimuth and elevation angles in radians. For simplicity, the azimuth origin is set to the radar frontal direction.

1.1. Detection constraint

The radar search pattern must ensure detection for a set of I missions. The parameters for each mission $i \in \mathcal{I} = \{1, \ldots, I\}$ are:

- σ_i the radar cross-section of the target.
- $R_{c,i} : \mathcal{A}_S \to \mathbb{R}^+$ the desired detection range. In our simulations, a mission desired detection range is defined by a minimum height $H_{\min}$ and a minimum distance $D_{\min}$, see Fig. 2:

$$R_{c,i}(az, el) = \begin{cases} D_{\min} & \text{if } el \leq \operatorname{asin}\left(\frac{H_{\min}}{D_{\min}}\right) \\ \frac{H_{\min}}{\sin(el)} & \text{otherwise} \end{cases} \tag{2}$$

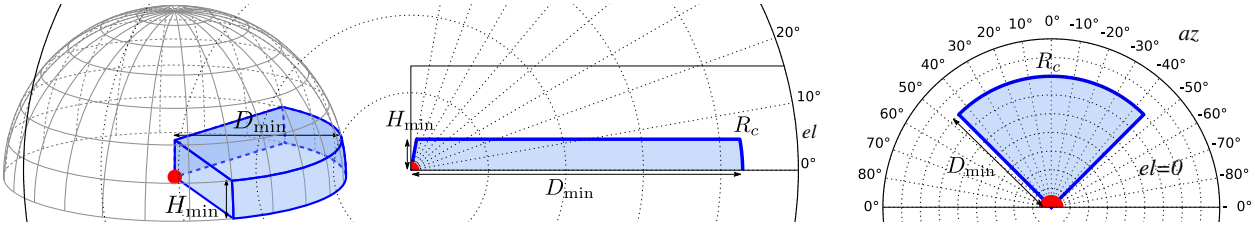

Fig. 2. *Desired detection range (left), azimuth cut (center), elevation cut (right)*

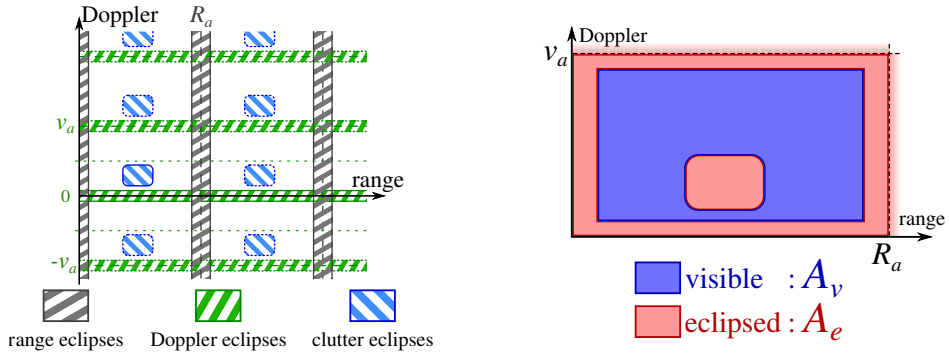

Fig. 3. *range-Doppler map with eclipses for given Doppler and range ambiguities (left) and its visible and occulted areas (right)*

- $S_{c,i} : \mathcal{A}_S \to \mathbb{N}$ be the desired scan update rate, which is the minimum number of scans to perform in a given direction during one radar search pattern.
- $SW_i \in \{0, \ldots, 4\}$ be the Swerling model [15].
- $P_d \in]0, 1[$ is the desired detection probability and $P_{fa} \in]0, 1[$ is the desired false alarm probability.

Information about the radar environment is also available:

- $\alpha : \mathcal{A}_S \to [0, 1[$ is the clutter eclipse coefficient. It represents the ratio of eclipsed area on the range-Doppler map in a given direction:

$$\alpha = \frac{A_e}{A_v + A_e} \tag{3}$$

  where A_v is the visible area and A_e is the eclipsed area, see Fig. 3.

- $\mu : \mathcal{A}_S \to \mathbb{R}^+$ is the terrain masking distance, i.e. the maximum detection range in a given direction before terrain masks block detection.

The radar search pattern ensures detection if for each mission $i \in \mathcal{I}$ and each direction $(az, el) \in \mathcal{A}_S$, the radar search pattern contains at least $S_{c,i}(az, el)$ dwells, each capable of detecting a target with radar cross-section σ_i at range $R_{c,i}(az, el)$ in direction (az, el), with at least detection probability P_d and at most false alarm probability P_{fa} in clutter eclipse coefficient $\alpha(az, el)$. In presence of terrain masking, desired detection range is replaced by $\min\{\mu, R_{c,i}\}$

The optimization problem is to minimize the time budget used by a radar search pattern validating the detection constraint previously described.

1.2. Dwell model

A dwell is the combination of a radiation pattern produced by the radar antenna, and a waveform signal generated by the radar and emitted by its antenna.

1.2.1. Radiation pattern: The radar antenna is modelled as a bidimensional linear phased-array, containing $K \times L$ isotropic radiating elements with horizontal spacing d_x and vertical spacing d_x. Phase and amplitude of each radiating element can be freely controlled:

$$a_{k,l} = A_{k,l}\, e^{j\phi_{k,l}} \tag{4}$$

with amplitude $A_{k,l} \in [0, 1]$, phase $\phi_{k,l} \in [0, 2\pi[$, and indexes $(k, l) \in \{1, ..., K\} \times \{1, ..., L\}$. The theoretical emission gain of the array antenna is [16]:

$$g_t(u, v) = \sum_{k=0}^{K-1} \sum_{l=0}^{L-1} a_{k,l}\, e^{j2\pi \frac{k d_y v + l d_x u}{\lambda}} \tag{5}$$

with λ the signal wavelength (which can be approximated by the waveform carrier), and with (u, v) the direction cosines coordinates derived from azimuth/elevation coordinates as

$$\begin{array}{rcl} u & = & -\cos(el)\sin(az) \\ v & = & \sin(el)\cos(t) - \sin(t)\cos(az)\cos(el) \end{array} \tag{6}$$

with t the array antenna tilt angle.
Azimuth and elevation are the usual coordinates for defining detection constraints, while direction cosines are the usual coordinates used for performing pattern analysis and synthesis. The reciprocal transformation of (6) is:

$$\begin{array}{rcl} az & = & \operatorname{atan2}\left(-u, \cos(t)\sqrt{1-u^2-v^2} - \sin(t)v\right) \\ el & = & \operatorname{asin}\left(\sin(t)\sqrt{1-u^2-v^2} + \cos(t)v\right) \end{array} \tag{7}$$

From this point on, we consider that functions defined on $\mathcal{A}_S$ can accept indiscriminately (u, v) and (az, el) as parameters, since variables can easily be substituted using (6) and (7).

The transformation between direction cosines and azimuth-elevation does not preserve areas. Informally, the transformation spreads surfaces in a non-uniform fashion, dispersing more power as the observation direction deviates from the array normal direction. This results in anisotropic scan losses:

$$L_s = \cos(\delta)^{-1} \tag{8}$$

where δ is the angle between the array antenna normal vector and the observation direction. Scan losses are squared in the radar equation since they occur at emission and reception.

1.2.2. Waveform: The radar can access a catalogue of available waveforms $\mathcal{W} = \{w_1, \ldots, w_P\}$. Each waveform $w \in \mathcal{W}$ in the catalogue has known characteristics and performances:

- signal wavelength: λ_w
- duration, which corresponds to the radar-time a dwell using waveform w would require for emission, reception and processing: T_w

- Signal-to-Noise Ratio detectability factor $s_w(i,\alpha)$ for given detection probability P_d and false alarm probability P_{fa} accounting for :
  - target type of mission i and its associated Swerling model [15].
  - clutter eclipse coefficient: α

Qualitatively, each waveform achieves a known compromise between its required processing time and its detection performances for a given target type in a given clutter configuration.

1.3. Detection range

The maximum detection range for mission i in direction (az, el) using dwell d with radiation pattern g_t and waveform w can be computed through the radar equation [17]:

$$R_{d,i}(az,el)^4 = \frac{P_m\, T_w\, g_t(az,el)\, g_r\, \lambda_w^2\, \sigma_i}{(4\pi)^3\, s_w(i,\alpha(az,el))\, L_u\, L_s(az,el)^2} \tag{9}$$

where P_m is the mean power of the radar, g_r is the reception gain of the narrow beam used in digital beam-forming, L_s are anisotropic scanned losses and L_u are uniform losses.

1.4. Reception processing

From (9), dwell d detection area for a given mission i is computed as:

$$\mathcal{A}_{d,i} = \{(az,el) \in \mathcal{A}_S,\ s.t.\ R_{d,i}(az,el) \geq R_{c,i}(az,el)\} \tag{10}$$

and its detection area for all missions is $\mathcal{A}_d = \bigcup_{i\in\mathcal{I}} \mathcal{A}_{d,i}$.

The radar performs digital beam-forming to sample the scanned area using simultaneous digital narrow beams. All digital narrow beams are supposed to have the same gain (except for a linear phase term used for beam-steering). The reception gain g_r is approximated as the broadside gain at half-power of the digital reception narrow beam.

The dwell scanned area size in direction cosines is limited by reception processing bandwidth. Thus the scanned area must be smaller than the maximum area the digital narrow beams can cover:

$$A_d = \text{number of reception beams} \cdot \text{digital beamwidth} \approx \iint_{\mathcal{A}_d} dudv \leq A_{\max} \tag{11}$$

1.5. General optimization problem formulation

Finding a radar search pattern $\mathcal{S}_{opt}$ ensuring the detection constraint over the surveillance space with minimal time-budget is a minimization problem under constraints:

$$\min \sum_{0\leq j\leq J} T_{w_j} \tag{12a}$$

$$s.t.\ \mathcal{S} = \{d_j = (g_j, w_j), 0 \leq j \leq J\},\ J \in \mathbb{N} \tag{12b}$$

$$\forall i \in \{0,\ldots,I\}, \mathcal{A}_S \subset \bigcup_{d\in\mathcal{S}} \mathcal{A}_{d,i} \tag{12c}$$

$$\forall d \in \mathcal{S},\ A_d = \iint_{\mathcal{A}_d} dudv \leq A_{\max} \tag{12d}$$

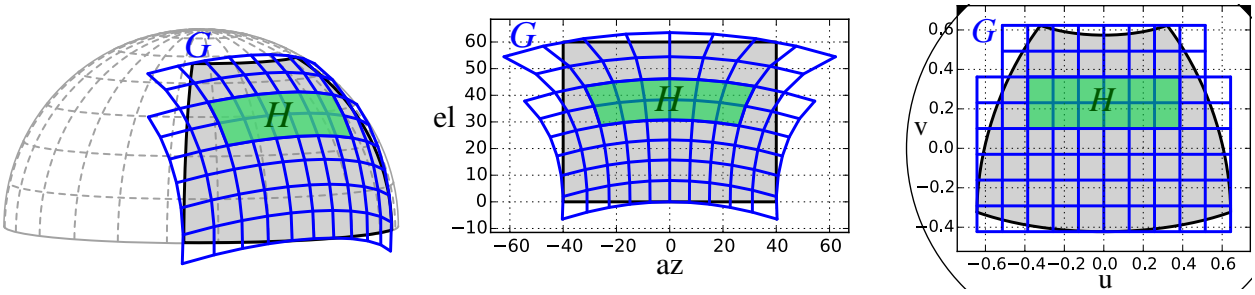

Fig. 4. *Detection grid G and a rectangle H in 3D (left), in azimuth/elevation (center), in direction cosines (right)*

The problem amounts to finding a radar search pattern $\mathcal{S}$ containing a finite number of dwells (12b), validating detection constraint over the entire surveillance space for all missions (12c), processable at reception (12d), and using minimal radar time-budget (12a).

2. Set Cover Problem Approximation

The general optimization problem is difficult to solve for several reasons: continuous variables in the phase-amplitude law of each dwell radiation pattern, mixed with discrete variables for each dwell waveform choice. Furthermore the number of variables is not set, as it depends on the number of dwells. Finally, the desired detection ranges $R_{c,i}$ are generally non-convex functions. It is thus a non-convex mixed optimization problem, with potentially a large number of variables. A more sensible way to tackle this problem is to approximate it as a combinatorial set cover problem, since it intuitively possesses a similar structure as a covering problem.

2.1. Discrete Detection Grid

The surveillance space in direction cosines coordinates is approximated by a finite bidimensional M-by-N regular grid, see Fig. 4. On this grid, the detection constraint is considered on each cell, with a finite number of cells, instead of working on the continuous set of possible azimuth-elevation directions.

Let $[u_{\min}, u_{\max}] \subset [0,1]$ and $[v_{\min}, v_{\max}] \subset [0,1]$ be the radar scanning range in direction cosines coordinates on the surveillance space. Let $M \in \mathbb{N}^*$ and $N \in \mathbb{N}^*$ define the desired grid resolution. Then the grid nodes are computed by :

$$\begin{array}{lll} u_0 = u_{\min}, & u_N = u_{\max} & u_n = u_0 + n\left(\frac{u_N - u_0}{N}\right) \\ v_0 = v_{\min}, & v_M = v_{\max} & v_m = v_0 + m\left(\frac{v_M - v_0}{M}\right) \end{array} \tag{13}$$

Any rectangle on grid G can be characterized by its upper left corner (u_n, v_m) and its lower right corner (u_q, v_r), see Fig. 4, with $0 \leq n < q \leq N$ and $0 \leq m < r \leq M$.

The number of possible rectangles on G is bounded by $\frac{MN(M+1)(N+1)}{4}$.
The problem is then divided into two parts:

- the generation, through pattern synthesis, of a collection of rectangular candidate dwells.
- the selection of an optimal subset among the rectangular candidate dwells.

2.2. Pattern Synthesis

Let H be a rectangle on grid G, characterized by nodes (u_n, v_m) and (u_q, v_r). The ideal radiation pattern covering H is

$$g_H(u,v) \propto \begin{cases} L_s(u,v)^2 \max_i \left\{ \frac{R_{c,i}(u,v)^4 s_w(i,\alpha)}{\sigma_i} \right\} & \text{if } u_n \leq u \leq u_q \text{ and } v_m \leq v \leq v_r \\ 0 & \text{otherwise} \end{cases} \tag{14}$$

up to a constant factor, as the array antenna feeds are normalized. This radiation pattern fits the maximum of among all missions' ideal energetic distributions. It is usually infeasible on a real antenna, because it features discontinuities on the rectangle edges, see Fig. 5. The radiation pattern is the Fourier transform of the antenna illumination law, see (5). A discontinuous radiation pattern would require an infinitely large antenna array. It corresponds to an infinite illumination law, similarly to a discontinuous time signal having an infinite spectrum: the instantaneous change of value in the signal indicates the presence of arbitrarily high frequencies.

A feasible radiation pattern $\hat{g}_H$ can be synthesized by applying a bidimensional Woodward-Lawson sampling method to the ideal pattern g_H, adapted from the one-dimensional method described in [16, 18]. Using sampled values of the desired pattern at given sampling points, the method synthesizes a feasible pattern that is guaranteed to hold the same values at the sampling points, see Fig. 5. The sampling points form a K'-by-L' grid with nodes $(u_l, v_k),\ 0 \leq l < L',\ 0 \leq k < K'$ (note that this grid has no relation to detection grid G) with:

$$\begin{array}{llll} L' & = 2\lfloor \frac{L}{2} \rfloor + 1, & u_l & = \frac{2l+1-L'}{L} \\ K' & = 2\lfloor \frac{K}{2} \rfloor + 1, & v_k & = \frac{2k+1-K'}{K} \end{array} \tag{15}$$

The number of sampling points along one dimension is the closest rounded-up odd number to the number of radiating elements on the same axis. The feeds of the feasible pattern are computed using the ideal pattern values at the sampling points:

$$\hat{a}_{k,l} = \frac{1}{KL} \sum_{k'=0}^{K'} \sum_{l'=0}^{L'} g_H(u_{l'}, v_{k'}) e^{-j\pi(k d_y v_{k'} + l d_x u_{l'})/\lambda} \tag{16}$$

The feeds are normalized: $\hat{a}_{k,l} \leftarrow \hat{a}_{k,l} / \max_{k,l}\{\hat{a}_{k,l}\}$ and Taylor filtering is used for decreasing sidelobes and Gibbs oscillations. From the feeds, the feasible pattern can be computed using (5).

Applying this synthesis procedure to all possible rectangles on grid G, with area inferior to the maximum processable area described in subsection 1.4, generates a collection of processable radiation patterns : $\mathcal{T} = \{\hat{g}_H, H \subset G\}$

Other synthesis methods based on least square optimization [19], genetic algorithms [20] and alternating projections [21] are also compatible with this approach.

2.3. Set Cover Problem

The set of candidate dwells $\mathcal{D}$ can be computed as the Cartesian product of $\mathcal{T}$, the set of synthesized radiation patterns, and $\mathcal{W}$, the set of available waveforms :

$$\mathcal{D} = \mathcal{T} \times \mathcal{W} = \{(g_t, w), g_t \in \mathcal{T}, w \in \mathcal{W}\} = \{d_1, \cdots, d_p\} \tag{17}$$

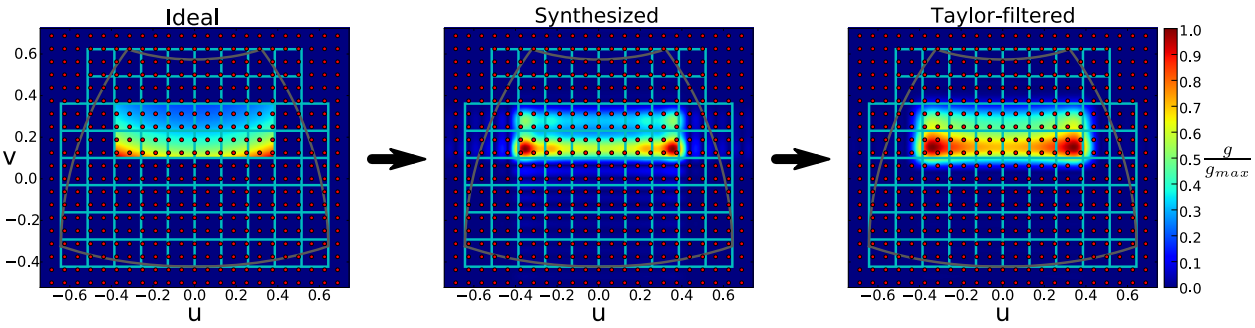

Fig. 5. *Ideal radiation pattern (left), synthesized radiation pattern (middle) and synthesized radiation pattern after Taylor filtering (right), with sampling points in red.*

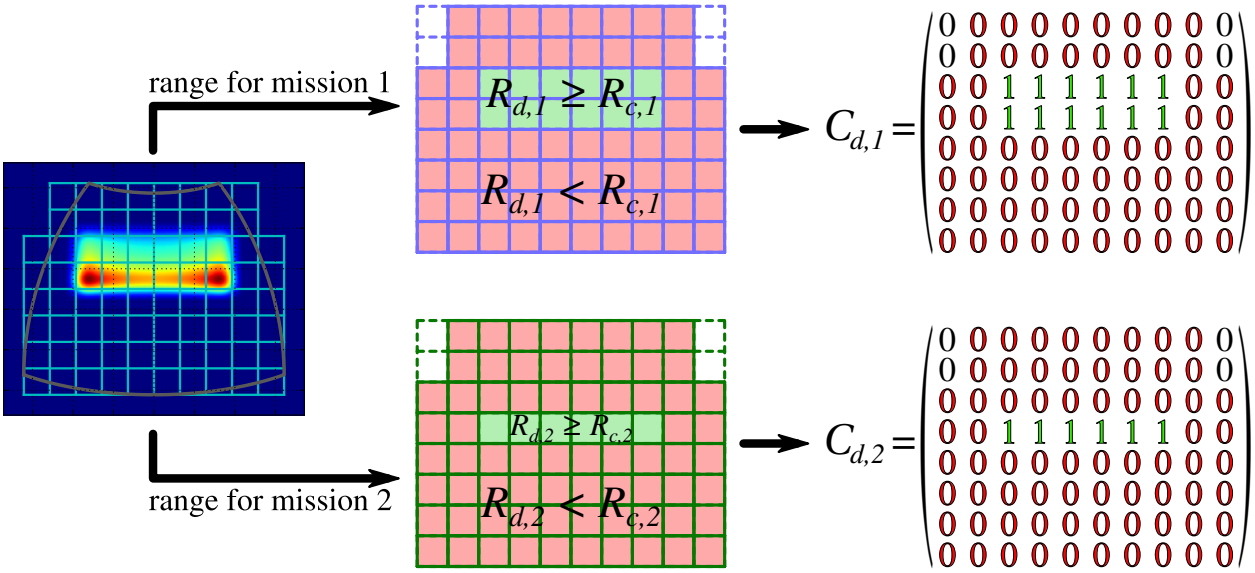

Fig. 6. *Computation of discrete covers for one dwell on two scanning missions*

For each dwell d_j in $\mathcal{D}$ and each mission i, see Fig. 6, dwell d_j discrete cover for mission i is computed by the formula:

$$C_{j,i}(m,n) = \begin{cases} 1 \text{ if } \forall (u,v) \in [u_n, u_{n+1}] \times [v_m, v_{m+1}], R_{j,i}(u,v) \geq R_{c,i}(u,v) \\ 0 \text{ otherwise} \end{cases} \tag{18}$$

where $R_{j,i}$ is dwell d_j detection range for mission i. Discrete cover $C_{j,i}$ represents the cells on which dwell d_j validates mission i detection constraint.

Dwells can have different covers for each mission, as energetic requirements differ between missions. Furthermore, some waveforms might be more efficient and suited for some missions. The minimum number of scans on each cell for mission i is defined as:

$$s_i(m,n) = \max_{\substack{u_n \leq u \leq u_{n+1} \\ v_m \leq v \leq v_{m+1}}} S_{c,i}(u,v) \tag{19}$$

Finding a radar search pattern validating detection constraints for all missions over the surveillance space amounts to finding a subset among candidate dwells whose sum of discrete covers

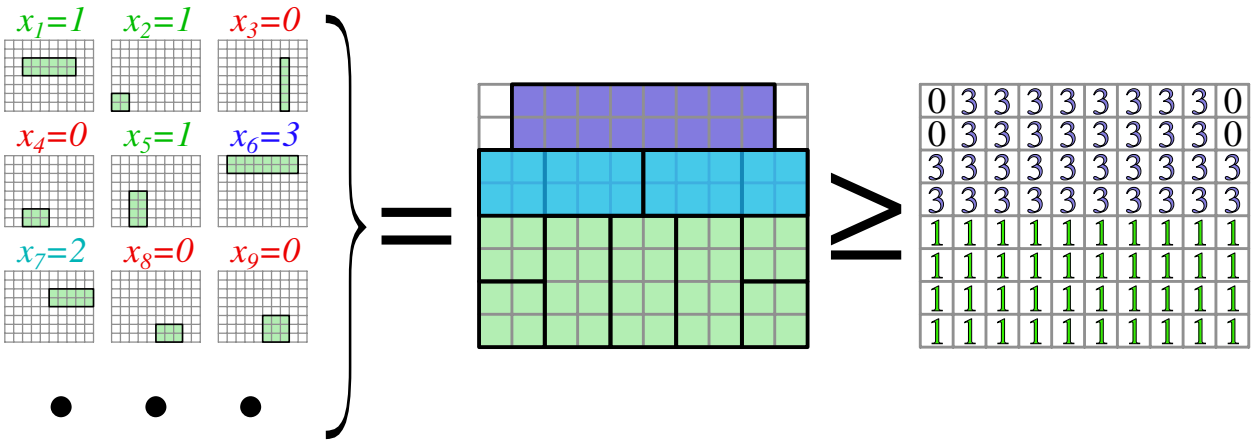

Fig. 7. *The set of available discrete covers with the chosen number of scan for each cover (left), the sum of the chosen discrete covers (middle) and the desired scan update rate for each cell (right)*

cover the entire grid G, with each cell $G(m,n)$ being covered by at least $s_i(m,n)$ dwells, see Fig. 7, for all missions.

With time-budget of the radar search pattern being the cost function of the optimization problem, the cost for each dwell d_j is its waveform duration T_w. It will be referred as T_j from now on.

Each dwell $d_j \in \mathcal{D}$ is associated to an integer selection variable x_j, indicating how many times dwell d_j is in the radar search pattern. Thus, the optimization problem (12) is approximated on grid G by the following set cover problem:

$$\begin{array}{ll} \min & \sum_{j=1}^{p} T_j x_j \\ s.t. & \forall i \in \{1,\dots,I\}, \forall (m,n),\ \sum_{j=1}^{p} x_j C_{j,i}(m,n) \geq s_i(m,n) \\ & \forall j \in \{1,\dots,p\}, x_j \in \mathbb{N} \end{array} \tag{20}$$

with p being the number of candidate dwells, i.e. the cardinal of set $\mathcal{D}$.

2.4. Integer Program

The approximation problem can be written as an integer program using matrix formulations: Let $\mathbf{x} = (x_1 \cdots x_p)^T$, let $\mathbf{T} = (T_1 \cdots T_p)^T$ and let

$$\mathbf{A}_i = \begin{pmatrix} C_{1,i}(0,0) & \cdots & C_{p,i}(0,0) \\ C_{1,i}(0,1) & \cdots & C_{p,i}(0,1) \\ \vdots & \ddots & \vdots \\ C_{1,i}(m,n) & \cdots & C_{p,i}(m,n) \\ \vdots & \vdots & \vdots \end{pmatrix}, \mathbf{A} = \begin{pmatrix} \mathbf{A}_1 \\ \vdots \\ \mathbf{A}_i \\ \vdots \\ \mathbf{A}_I \end{pmatrix}, \mathbf{s}_i = \begin{pmatrix} s_i(0,0) \\ s_i(0,1) \\ \vdots \\ s_i(m,n) \\ \cdots \end{pmatrix} \text{ and } \mathbf{s} = \begin{pmatrix} \mathbf{s}_1 \\ \vdots \\ \mathbf{s}_i \\ \vdots \\ \mathbf{s}_I \end{pmatrix} \tag{21}$$

Let $s_{\max}$ be the maximum value of vector $\mathbf{s}$. Then the approximation problem can be written as:

$$\begin{array}{ll} \min & \mathbf{T}^T.\mathbf{x} \\ s.t. & \mathbf{A} \cdot \mathbf{x} \geq \mathbf{s} \\ & \mathbf{x} \in \{0, \cdots, s_{\max}\}^p \subset \mathbb{N}^p \end{array} \tag{22}$$

3. Optimization Algorithm

Generally, integer programs are difficult to solve in a straightforward manner. Currently, no algorithm for computing quickly an optimal solution is known, and most methods rely on some form of exploration of the set of possible solutions. While the size of the solution space is finite, it grows exponentially with the number of variables and is usually huge: for the problem described in the previous sections, there are $(1 + s_{\max})^p$ possible solutions.

Combining branch-and-bound exploration with relaxation methods can be used to avoid exhaustive enumeration of all possible solutions, by breaking down the integer program into easier sub-problems. However, the computational cost of this approach can still be important depending on the problem instance.

3.1. Linear Relaxation

By removing the integer constraint, and allowing the integer vector $\mathbf{x}$ to take any real positive value, the integer program is turned into a linear program:

$$\begin{array}{ll} \min & \mathbf{T}^T.\mathbf{x} \\ s.t. & \mathbf{A} \cdot \mathbf{x} \geq \mathbf{s} \\ & \mathbf{x} \in [0, s_{\max}]^p \subset \mathbb{R}^p \end{array} \tag{23}$$

Unlike integer programs, linear programs can be solved in pseudo-polynomial time, and have very efficient practical algorithms, such as Dantzig's simplex method [22].

In linear programs, each inequality constraint defines a hyperplane being the limit between the half-space of valid solutions and the half-space of invalid solutions for said constraint. The intersection of all valid half-spaces generates the set of feasible solutions for the linear program, and forms a convex polyhedron. The polyhedron convexity permits use of descent methods. This is not possible for integer programs, since integer solutions are isolated points in the feasible convex polyhedron.

Dantzig's simplex method moves between vertices on the convex polyhedron, decreasing the cost function at each step, until reaching a vertex with no decreasing neighbor; yielding by convexity an optimal solution [22]. The relaxed optimal solution $\mathbf{x}^*_{LP}$ may contain non-integer values. Thus $\mathbf{x}^*_{LP}$ might not necessarily correspond to a radar search pattern, but it produces a lower bound of the minimum time budget of an optimal radar search pattern.

3.2. Branch-and-Bound Method

A finite tree is used to represent all possible solutions of the integer program [23]. Each node represents the choice of a value for an integer variable, see Fig. 8, and has $1 + s_{\max}$ children. Each end leaf represents a solution for the integer program, when all variables have been set.

At each node, it is possible to estimate a lower bound of the node sub-tree best solution, by solving the linear relaxation of the non-set variables. Exploration of certain sub-trees can be avoided if their lower bound is higher or equal to the best current solution. The method takes its name from the two steps describing it:

- Branching: Each branch at the current node (with depth $i-1$) correspond to a different chosen value for the next variable x_i. In each branch, x_i is no longer a variable but a parameter. The

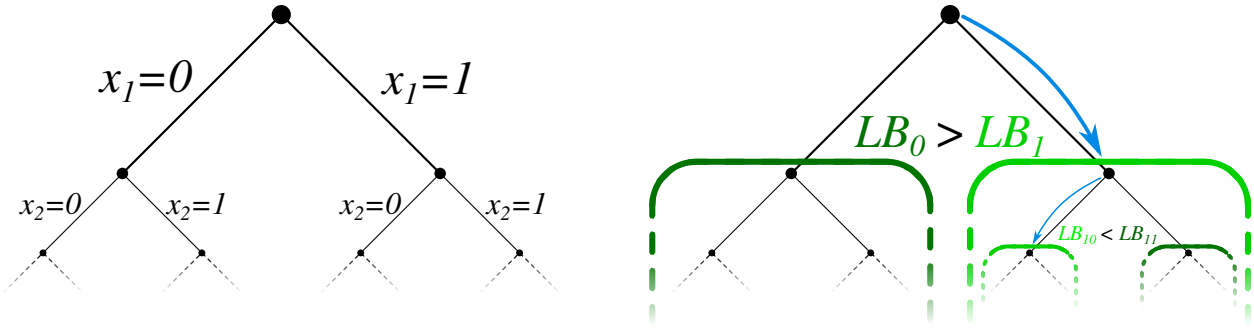

Fig. 8. *Finite tree of solutions with* $s_{\max} = 1$ *(left) and branch-and-bound method (right)*

current problem is thus divided into $(1 + s_{\max})$ smaller sub-problems, each considering a different value for x_i and each having one less variable.

- Bounding: The current problem is relaxed into a linear program, whose solution is a lower bound of the current problem best solution. Depending on the lower bound value, the node sub-tree will be explored next (if it is the most promising branch), later (if there is a more promising branch), or never (if a better solution has already be found in another branch).

There are many variants of branch-and-bound, relying on different criteria for defining the exploration order of the nodes [23], or using other relaxation methods with different trade-offs between speed and tightness of the lower bound [14].

Mixed-integer linear programs solvers are heavily optimized and rely on various heuristics to define the exploration strategy and improve bound estimations.

Branch-and-bound offers several advantages in regards to engineering design and real-time applications:

- "Gap-to-optimality" estimation: the method produces and refines a lower bound on the optimal objective value. This bound can be used to measure how far from optimality a feasible solution is.
- "Just-in-time" solution: the method explores the tree of possible solutions while keeping track of the best solution(s) found so far. "Just-in-time" solution(s) can be produced for real-time applications without waiting for optimal convergence.
- Multiple solutions generation: a population of solutions can generated during the exploration. Various criteria can be defined to filter the population: population size, maximum gap-to-optimality, maximum objective value...

4. Implementation and results

4.1. Simulation

The approximation procedure described in this article was applied to a study case with two scanning missions in presence of localized clutter and terrain masking with a 3× scan update rate constraint above the terrain mask, see Fig. 9.

The radar array antenna has 30×30 half-spaced radiating elements. The grid G is laid on a 20×20 lattice. The radar has two available waveforms $\mathcal{W} = \{w_1, w_2\}$, with a long waveform w_1

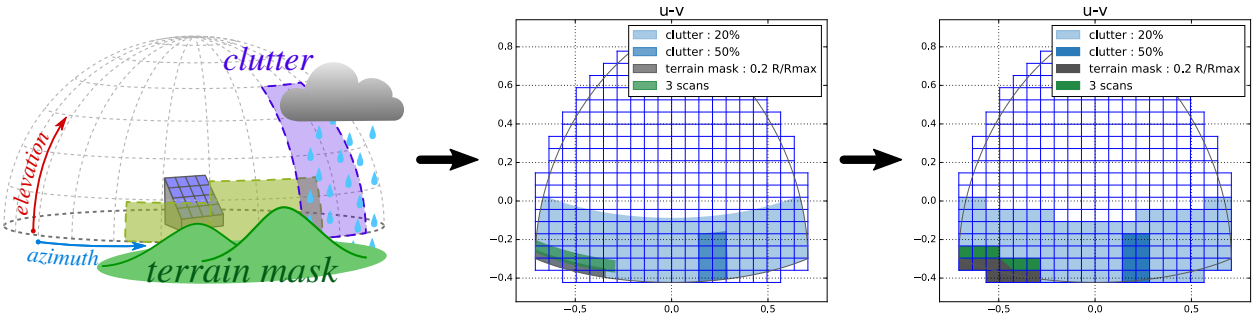

Fig. 9. *Mission constraints in azimuth-elevation (left), direction cosines (center) and discrete mission constraints (right)*

and a short waveform w_2. The approximation procedure produced 11282 feasible dwells. The detection grid contains 326 cells for both scanning missions. The corresponding integer program has 11282 variables and 652 inequality constraints.

The integer program is computed using Python, and optimization is done with CPLEX [24]. Total computation time for finding one optimal solution is 36 seconds on an i7-3770@3.4GHz processor with a memory usage of 452MB.

The optimal radar search pattern found contains 20 dwells, see Fig. 11, and combines overlapping dwells to achieve the desired global scan update rate, while ensuring the detection range on both missions.

However, this optimal solution is not unique. Alternative optimal solutions exists, see Fig. 10, Fig. 11, Fig. 12). In 130 seconds, the solver found 440 different optimal solutions. The list is not exhaustive, and it seems likely that many other combinations exist:

- Every solution has the same cost, and use exactly 20 dwells: 14 with a short waveform and 6 with a long waveform.
- Among those, 7 dwells (2 with short waveform and 5 with long waveform) are the same for all optimal solutions found. Those dwells form an *invariant of optimality*.
- The remaining 13 dwells (always 12 with short waveform and 1 with long waveform) are always drawn from a subset of 261 possible dwells (254 with short waveform and 7 with long waveform).

Informally, the *invariant of optimality* represents the constraining part of an optimal solution, while different combinations can be chosen for the remaining dwells among the pool of 261 dwells used in optimal solutions. There are probably more possible solutions as many different combinations among the 261 dwells can produce new solutions.

The invariant of optimality mostly consists of low-elevation dwells with long waveform. The low-elevation area of surveillance space contains the most restrictive detection constraints for the cover. While the high-elevation area, with inferior energetic requirements, offers several possibilities for optimal covering.

4.2. Comparison to a pencil-beam lattice

The optimized search pattern was compared to a pencil-beam rectangular lattice, which uses narrow beams with short dwells. Each beam has a different dwell frame time, minimized for the

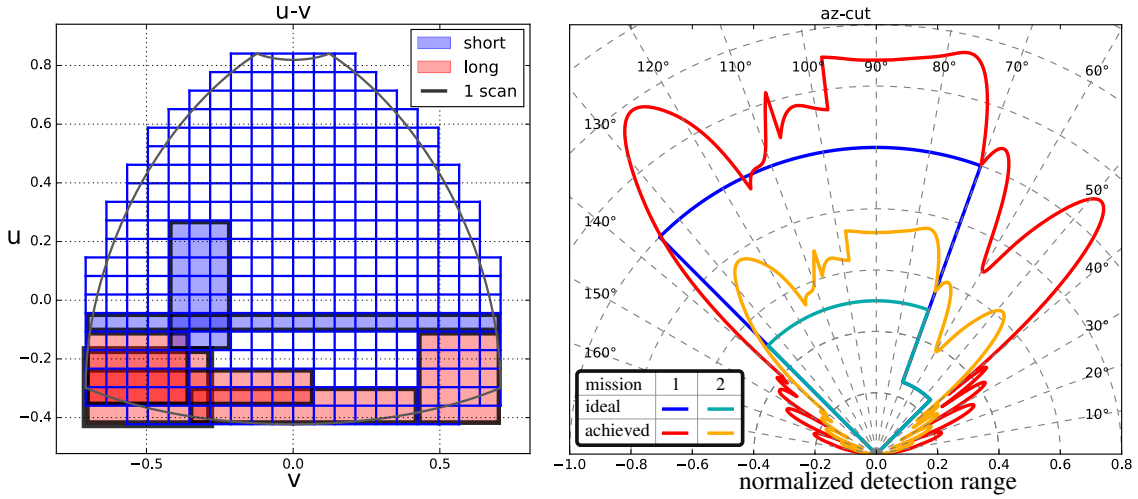

Fig. 10. *Invariant part of the optimal solutions and detection range on the horizon* ($elevation = 0$)

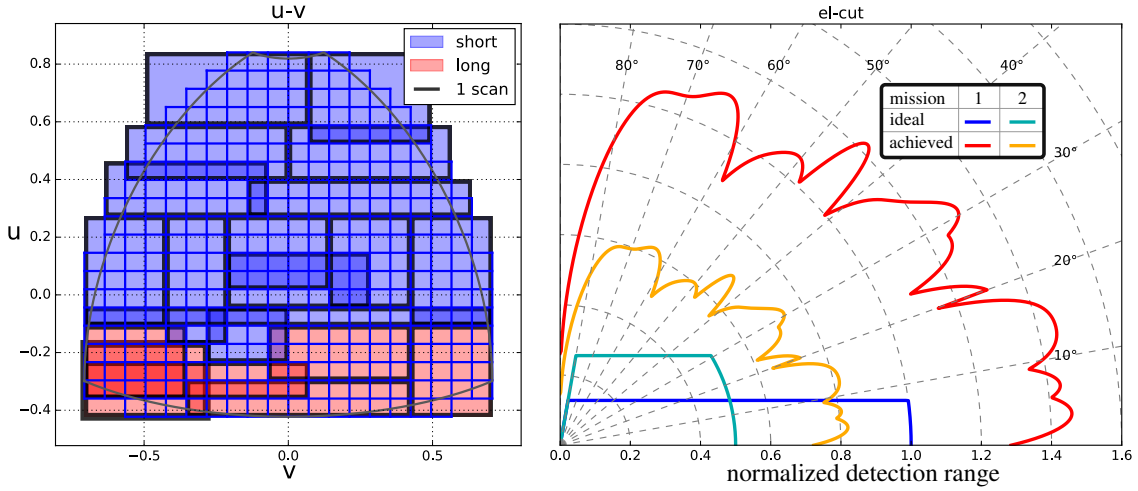

Fig. 11. *One possible complete optimal solution and the detection range in elevation* ($azimut = 0$)

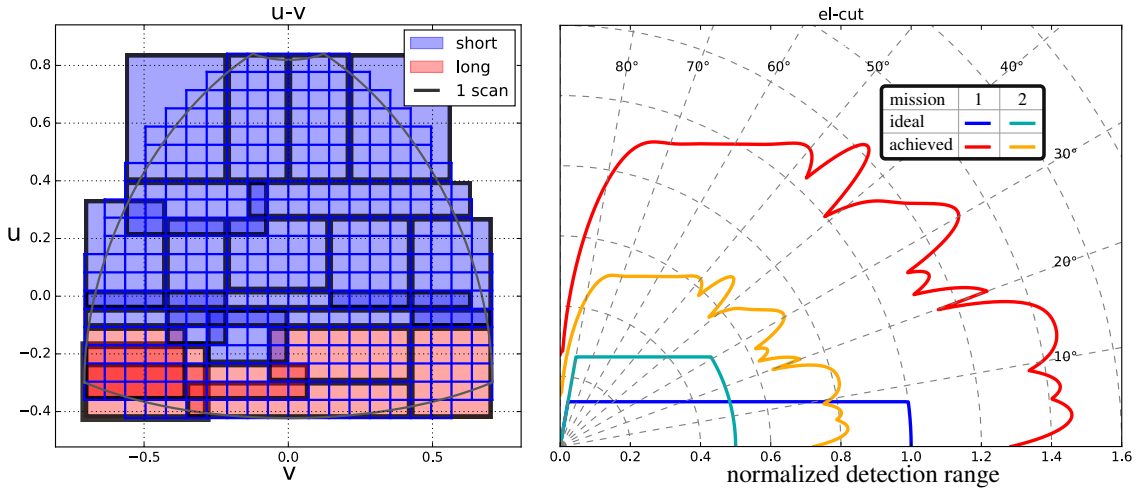

Fig. 12. *A second possible optimal solution and the detection range in elevation* ($azimut = 0$)

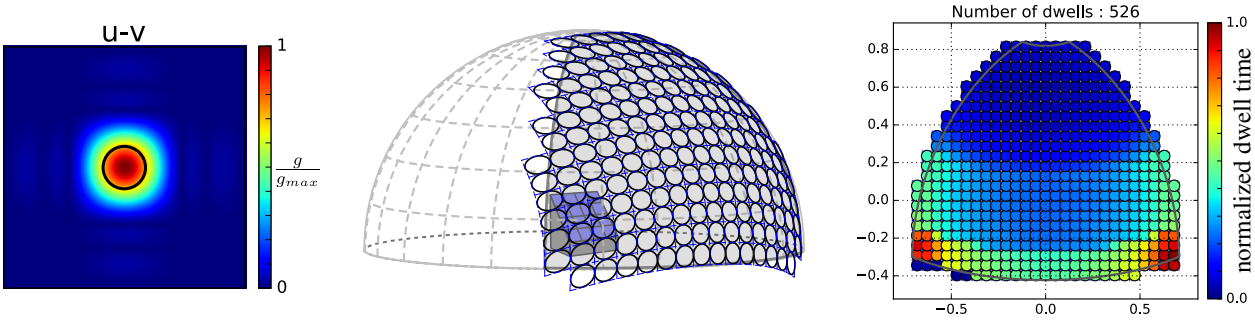

Fig. 13. *Pencil-beam (left), lattice of pencil-beams (center) and dwell duration for each pencil-beam (right)*

mission requirements, see Fig. 13. However, those dwells frame time is generally too short to efficiently account for eclipses. The pencil-beam lattice typically requires multiple scans for achieving the detection requirements defined in subsection 1.1.

The time-budget of the optimized search pattern is 27% lower than the average time-budget of the pencil-beam rectangular lattice, and is 47% lower than the worst-case time-budget of the pencil-beam rectangular lattice. The optimized search pattern advantage comes from the use of longer waveform, which are more efficient at dealing with clutter.

5. Conclusions

While providing a natural framework for radar search pattern optimization, the approximation procedure originally presented in [11] is shown to be flexible and can account for additional constraints, such as multiple missions, localized clutter, terrain masking and direction specific scan update rate constraints. This flexibility is due to the approximation procedure, which separate a complicate problem into consecutive simpler steps: grid discretization, pattern synthesis and dwell selection. The generic nature of integer programs for optimizing decision problems can integrate those constraints while preserving the mathematical structure of the optimization problem.

This framework will become a useful tool to help engineers in designing and optimizing radar search patterns. A significant advantage of this approach is its suitability for real-time applications. As the branch-and-bound method explores the solution space, it can return any improving solution as soon as found and then resume the optimization. The optimality gap provides information regarding the best improvement to be expected from any future solution. This method is thus particularly fit for providing "just-in-time" solutions.

Acknowledgements

This work is partly supported by a DGA-MRIS scholarship.

References

[1] F. Barbaresco, P. O. Gaillard, T. Guenais, N. Harvey, M. Johnston, B. Monnier, P. Sims, R. Wills. "Intelligent radar management by advanced beamscheduling algorithms based on

short-time planning constraints relaxation strategies", *IEEE International Symposium on Phased Array Systems and Technology, 2003.*, pp. 283–288, (2003).

[2] F. Barbaresco, J. Deltour, G. Desodt, B. Durand, T. Guenais, C. Labreuche. "Intelligent m3r radar time resources management: Advanced cognition, agility & autonomy capabilities", *Radar Conference - Surveillance for a Safer World, RADAR. International*, (2009).

[3] M. I. Jimenez, L. D. Val, J. J. Villacorta, A. Izquierdo, M. R. Mateos. "Design of task scheduling process for a multifunction radar", *IET Radar, Sonar Navigation*, **6(5)**, pp. 341–347, (June 2012).

[4] S. L. C. Miranda, C. J. Baker, K. Woodbridge, H. D. Griffiths. "Comparison of scheduling algorithms for multifunction radar", *IET Radar, Sonar Navigation*, **1(6)**, pp. 414–424, (Dec 2007).

[5] P. W. Moo. "Scheduling for multifunction radar via two-slope benefit functions", *IET Radar, Sonar Navigation*, **5(8)**, pp. 884–894, (Oct 2011).

[6] V. Jeauneau. "Contribution à l'ordonnancement temps réel - application aux radars multifonctions", Ph.D. thesis, Université Pierre et Marie Curie (UPMC), (2013).

[7] V. Jeauneau, F. Barbaresco, T. Guenais. "Radar tasks scheduling for a multifunction phased array radar with hard time constraint and priority", *Radar Conference (Radar), International*, (2014).

[8] P. M. Hahn, S. D. Gross. "Beam shape loss and surveillance optimization for pencil beam arrays", *IEEE Transactions on Aerospace and Electronic Systems*, **AES-5(4)**, pp. 674–675, (1969).

[9] D.-S. Jang, H.-L. Choi, J.-E. Roh. "Search optimization for minimum load under detection performance constraints in multi-function phased array radars", *Aerospace Science and Technology*, **40**, pp. 86–95, (2015).

[10] S. Torres, R. Adams, C. Curtis, E. Forren, D. Forsyth, I. Ivic, D. Priegnitz, J. Thompson, D. Warde. "A demonstration of adaptive weather surveillance and multifunction capabilities on the National Weather Radar Testbed Phased Array Radar", *Radar Conference (Radar), 2014 International*, (2014).

[11] Y. Briheche, F. Barbaresco, F. Bennis, D. Chablat, F. Gosselin. "Non-uniform constrained optimization of radar search patterns in direction cosines space using integer programming", *2016 17th International Radar Symposium (IRS)*, (2016).

[12] Y. Briheche, F. Barbaresco, F. Bennis, D. Chablat. "Optimization of radar search patterns for multiple scanning missions in localized clutter", *2016 IEEE Conference on Antenna Measurements Applications (CAMA)*, pp. 1–4, (2016).

[13] V. V. Vazirani. *Approximation Algorithms*, (Springer-Verlag New York, Inc., 2001).

[14] B. Yelbay, Ş. İ. Birbil, K. Bülbül. "The set covering problem revisited: An empirical study of the value of dual information", *Journal of Industrial and Management Optimization*, **11(2)**, pp. 575–594, (2015).

[15] P. Swerling. "Probability of detection for fluctuating targets", *IRE Transactions on Information Theory*, **6(2)**, pp. 269–308, (1960).

[16] W. Stutzman, G. Thiele. *Antenna Theory and Design*, (Wiley, 2012).

[17] M. Skolnik. *Radar Handbook, Third Edition*, (McGraw-Hill Education, 2008).

[18] S. J. Orfanidis. *Electromagnetic Waves and Antennas*, (Rutgers University, 2016), [Online]. Available: http://www.ece.rutgers.edu/~orfanidi/ewa/.

[19] B. D. Carlson, D. Willner. "Antenna pattern synthesis using weighted least squares", *IEE Proceedings H (Microwaves, Antennas and Propagation)*, volume 139, pp. 11–16, (IET, 1992).

[20] G. K. Mahanti, A. Chakraborty, S. Das. "Phase-only and amplitude-phase only synthesis of dual-beam pattern linear antenna arrays using floating-point genetic algorithms", *Progress In Electromagnetics Research*, **68**, pp. 247–259, (2007).

[21] Y. Han, C. Wan. "Scalable Alternating Projection and Proximal Splitting for Array Pattern Synthesis", *International Journal of Antennas and Propagation*, (2015).

[22] J. Matouek, B. Gärtner. *Understanding and Using Linear Programming (Universitext)*, (Springer-Verlag New York, Inc., Secaucus, NJ, USA, 2006).

[23] M. Conforti, G. Cornuejols, G. Zambelli. *Integer Programming*, (Springer Publishing Company, Incorporated, 2014).

[24] "IBM ILOG CPLEX Optimization Studio, v12.6", http://www-03.ibm.com/software/products/en/ibmilogcplestud/, (2015).